Supplement of Saf. Nucl. Waste Disposal, 2, 69–70, 2023
https://doi.org/10.5194/sand-2-69-2023-supplement
© Author(s) 2023. CC BY 4.0 License.

Supplement of

The anisotropy of geomaterial granite

Franz Müller et al.

Correspondence to: Franz Müller (f.mueller@geo.tu-freiberg.de)

The copyright of individual parts of the supplement might differ from the article licence.

The anisotropy of geomaterial granite

Franz Müller[1], Peter Hallas[2], Uwe Kroner[1]
[1]Institut für Geologie, TU Bergakademie Freiberg, Bernhard-von-Cotta Str. 2, 09599 Freiberg, Germany
[2]Thüringer Landesamt für Umwelt, Bergbau und Naturschutz, Außenstelle Weimar, Dienstgebäude 2, Carl-August-Allee 8–10, 99423 Weimar, Germany

Introduction

Granites represent suitable crystalline host rocks for nuclear waste repositories because of their mechanical strength and apparent isotropy. Despite their optical appearance, granites show a primary structural anisotropy (Bouchez, 1997) that evolved during emplacement and crystallization of the melt. Major processes involved are magmatic flow and oriented crystal growth (Müller et al., 2011). It is likely that primary anisotropic petrophysical properties control the orientation of post-magmatic structural features like extensional fractures, and thus, may shape potential fluid pathways.

We present the first results of a systematic study of felsic plutonites, i.e., the **GAME-project** (*"Gefüge-, Textur- und Anisotropie-Messungen von potenziell für die Endlagerung geeigneten Graniten zur Charakterisierung möglicher Fluidwegsamkeiten"*).

Methods

To estimate the rocks primary anisotropies, we analyzed the **crystallographic preferred orientation (CPO)** of the rock-forming minerals. CPOs were measured using the neutron time-of-flight (ToF) texture diffractometer "SKAT" and electron backscatter diffraction (EBSD).

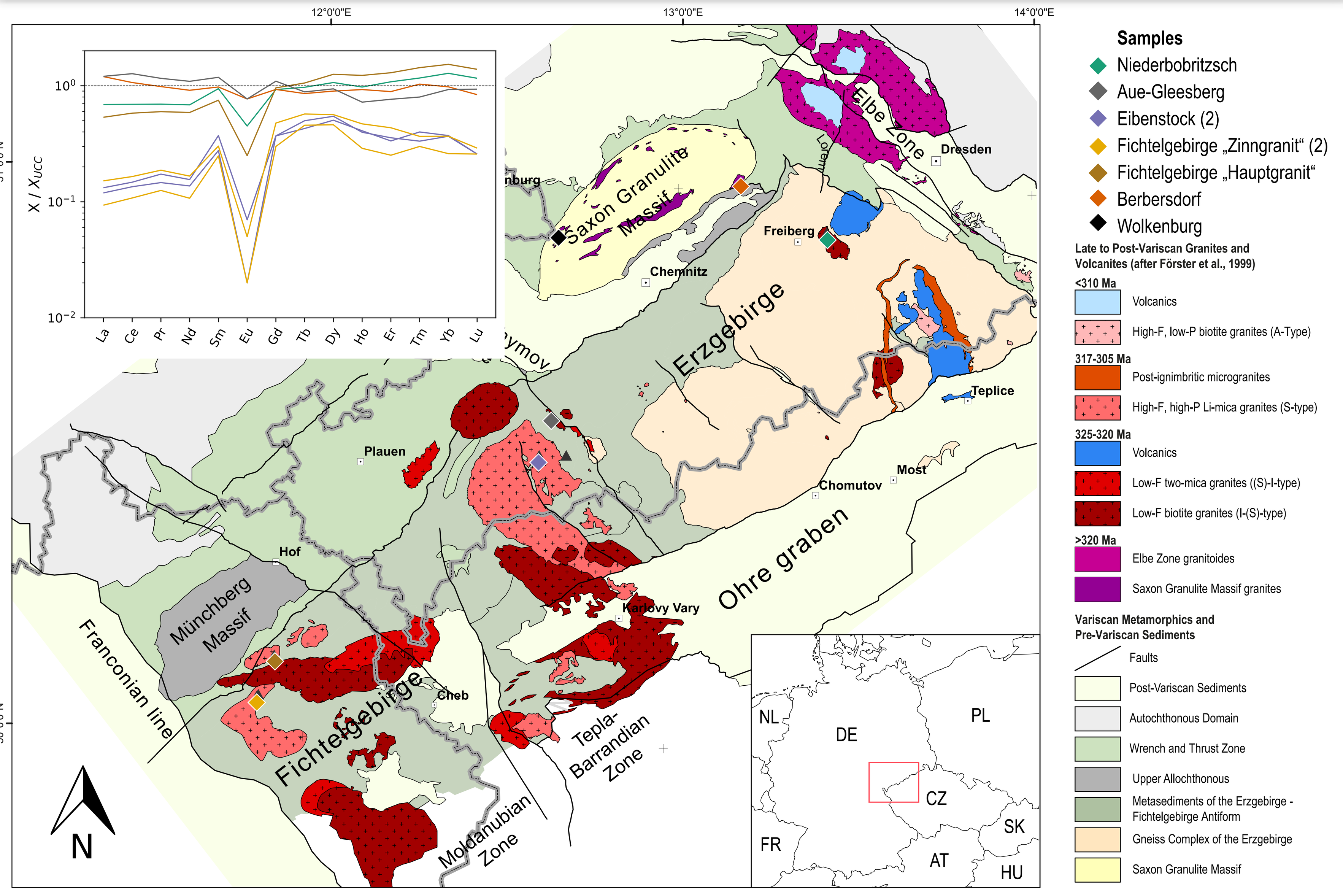

Fig. 1: Geological map of the sampling area (Erzgebirge-Fichtelgebirge Complex, NW-Bohemian Massif). Subdivision of granites after Förster et al, 1999 and of metamorphics after Kroner et al., 2007; Hallas et al., 2021.

Neutron-ToF: Texture analysis of very low-strain granites

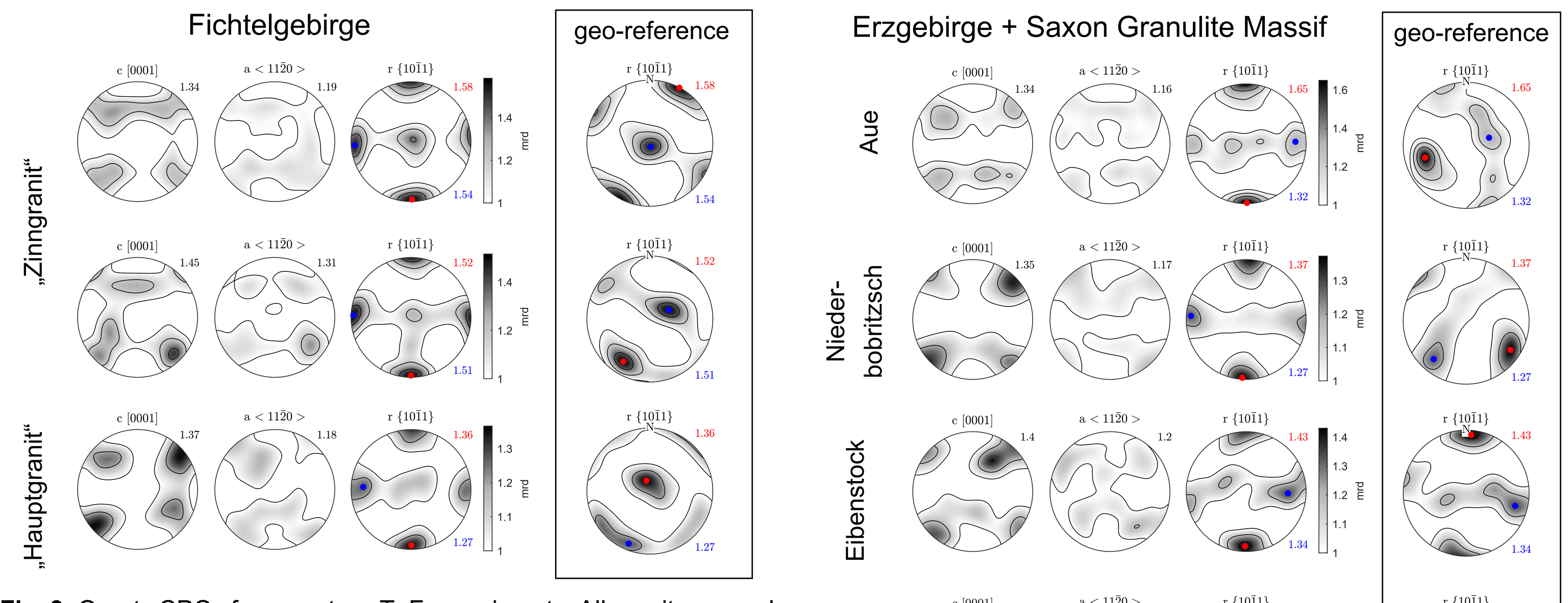

Fig. 3: Quartz CPOs from neutron-ToF experiments. All granites reveal similar and symmetrical CPO's with point maxima of the positive rhombs (maximum marked red, minimum in blue). In geographical reference-frame the positive rhombs are oriented subhorizontally at variable orientations but coherent at a local scale (see Fichtelgebirge).

Whole-rock anisotropy (Berbersdorf)

Calculation of anisotropic elastic rock properties from whole-rock texture data (Mainprice et al., 2011):

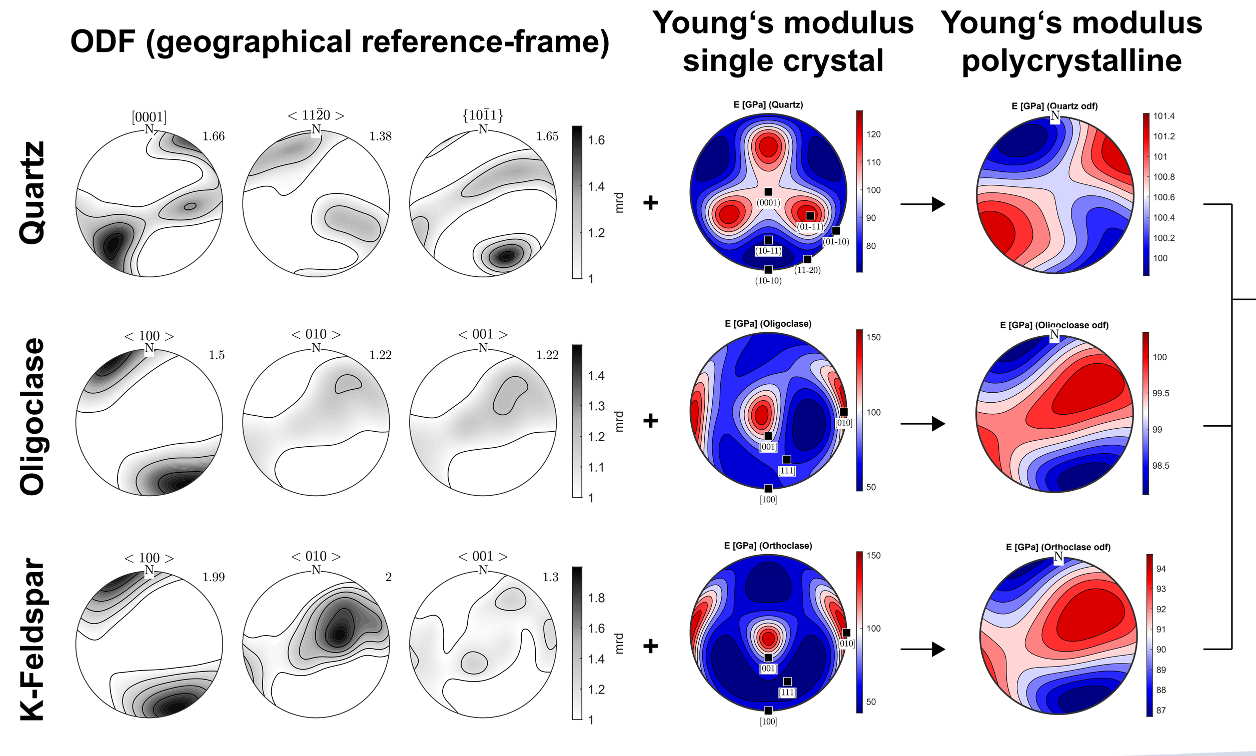

Fig. 4: Example of the **calculation of the Young's modulus of Berbersdorf granite**. ODF's and elastic stiffness tensors (single crystal) are used to calculate a polycrystalline average. The Vol.- % weighted total of these phase-specific tensors produces the whole-rock average.

Samples & Fabrics

- late-Variscan felsic plutons from three sites (**Erzgebirge, Saxon Granulite Massif and Fichtelgebirge**, see Fig. 1): different tectonic settings during intrusion
- different stages of fractionation of the peraluminous granite suites

Plagioclase + K-feldspar:
- often zonated + crystal-mush structures
- xeno- to hypidiomorphic grains with small aspect-ratios
- no signs of ductile/brittle-ductile deformation

Quartz:
- near- to subsolidus growth with xenomorphous grain boundaries
- low-strain, low-temperature deformation: diffusion creep, undulose extinction, deformation lamellae, bulging
- Saxon Granulite Massif granites show variable degrees of grain boundary migration recrystallization (high-T)

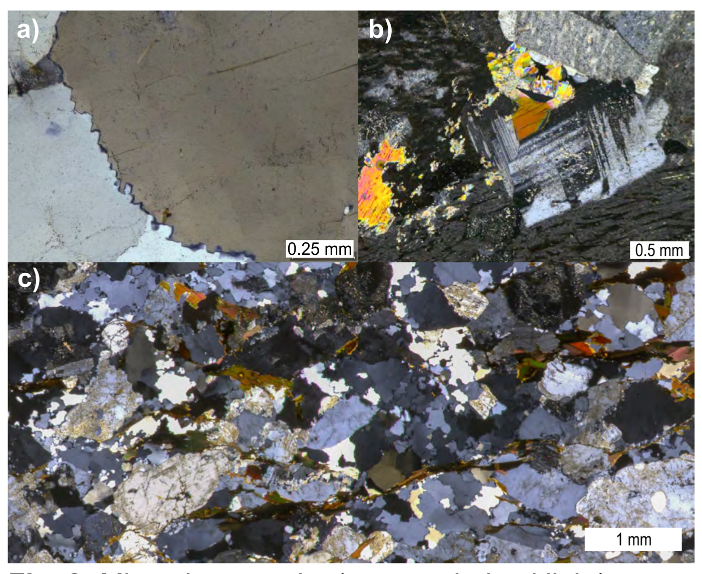

Fig. 2: Microphotographs (cross-polarized light).
a) Bulging quartz (Fichtelgebirge „Zinngranit").
b) Intergrown plagioclase crystals (Eibenstock).
c) Grain boundary migration recrystallized quartz grains (Wolkenburg).

EBSD

EBSD at very low magnification (Yamamoto et al., 2010) allows for spatially resolved texture measurement of large areas covering significant numbers of mineral grains.

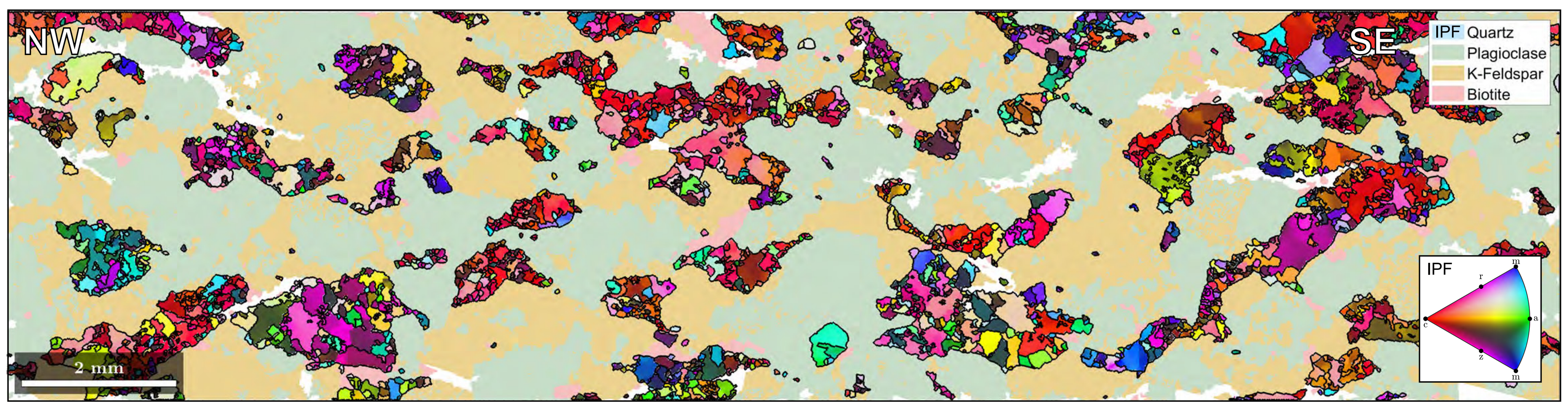

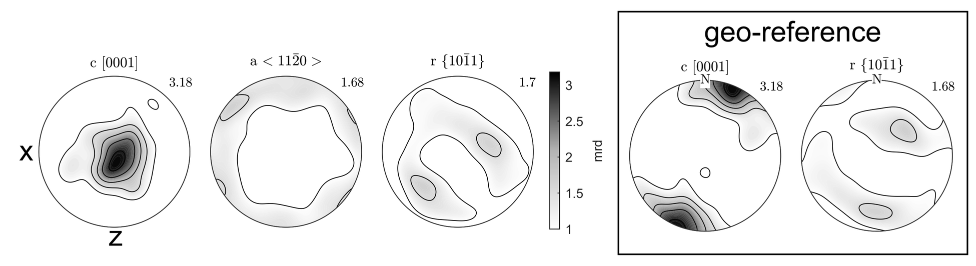

Fig. 5: Wolkenburg Granite. EBSD-map and Quartz Polefigures (xz-plane of the finite strain ellipsoid and geographical reference frame, Quartz inverse polefigure colors for y-direction, upper hemisphere).
The syn-kinematic granite intruded into the Shearzone of the hanging-wall of the Saxon Granulite Massif (top to SE). The Quartz CPO with a **c-axis maximum in Y represents a high-temperature, low-strain texture** that is in contrast to the other granite samples.

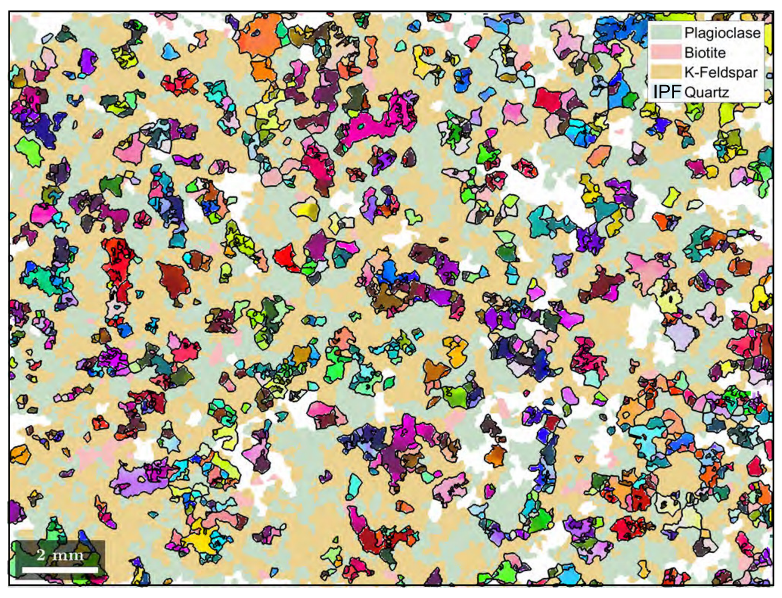

Neutron-ToF results can be reproduced with EBSD (Fig. 6 and 3). Typical difficulties in measuring granite textures, i.e. weak CPOs and large grainsizes, are overcome by measuring large areas.

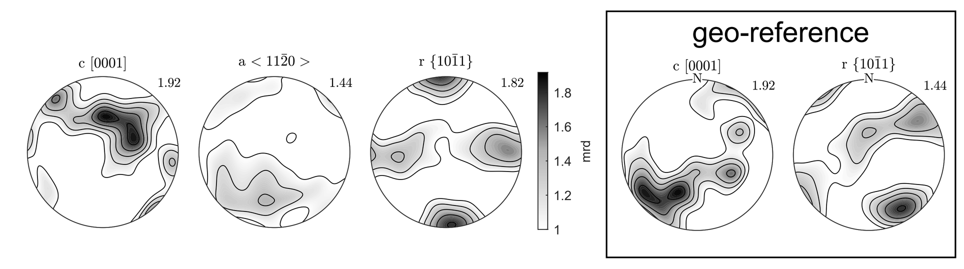

Fig. 6: Berbersdorf Granite. EBSD-map and Quartz Polefigures (rotated for symmetrical representation and for geographical reference-frame, upper hemisphere, Quartz inverse polefigure colors for vertical polefigure direction).

First Results

Methodology:
Low-magnification EBSD is able to substitute neutron-diffraction experiments for granite texture measurements, with higher availability and cost-efficiency.

Primary Anisotropy:
- **all low-strain granites share a common, orthotropic symmetrical, quartz CPO (Fig. 3)**:
  - point maxima of the positive rhombs ({10-11}) and a perpendicular girdle
  - c-axes ([0001]) small-circle girdle
- Orthotropic **quartz CPOs show preferred geographical alignment** on the local scale (Fichtelgebirge, Fig. 3)
- High-T, low-strain, plastic deformation **(grain boundary migration) overprints preexisting CPO** (Saxon Granulite Massif, Fig. 5, 6)
- the **Quartz-CPO can be explained by two perpendicular axial-rotational distributions of the positive rhombs** (Fig. 7)
- feldspar CPOs dominate the calculated whole-rock elastic anisotropy (Fig. 4)

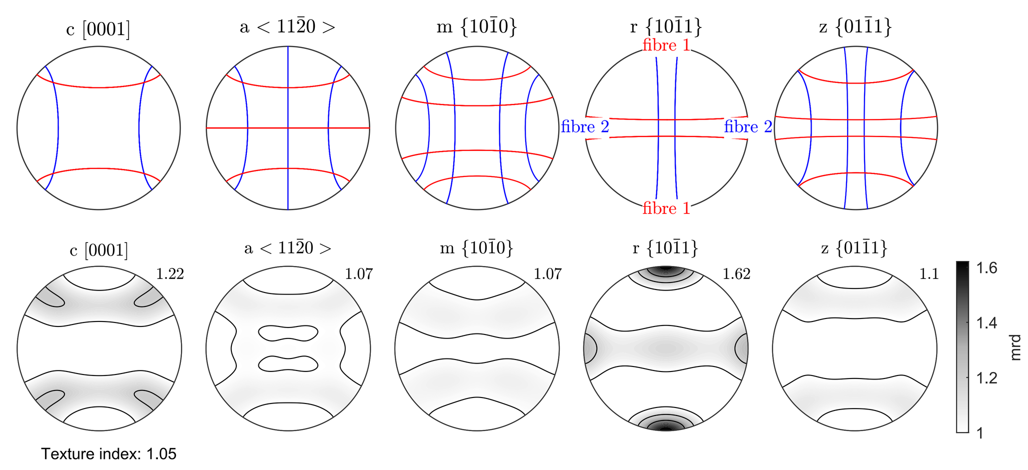

Fig. 7: The odf-model for low-strain granites is composed of a uniform portion, a vertical fibre-odf of {10-11} (red) and a weaker horizontal fibre-odf of {10-11} (blue). Combined model-odf with half-width of 20° below.
Fibre-orientations correspond to the point-maxima orientations of the positive rhombs in Fig. 3.

Project outlook

Quantity:
- **large number of samples**, covering a larger structural variety and more magmatic and tectonic settings

Primary Anisotropy:
- **spatially resolved texture measurements (EBSD)** allow for the investigation of texture-forming processes
- **AMS (Anisotropy of Magnetic Susceptibility)**: Quantitative fabric description (SPO)

Late- to Postmagmatic (Secondary) Anisotropy:
- **structural analysis of annealed and open microcracks** (uiversal-stage, image analysis)
- uni-/trixial **pressure tests** oriented according to the recent stress-field ('finite anisotropy')

References

Bouchez, J. L. (1997). Granite is never isotropic: An introduction to AMS studies of granitic rocks. Granite: From Segregation of Melt to Emplacement Fabrics. J. L. Bouchez, D. H. W. Hutton and W. E. Stephens. Dordrecht, Springer.
Forster, H.-J., et al. (1999). "Late-Collisional Granites in the Variscan Erzgebirge, Germany." Journal of Petrology 40(11): 1613–1645.
Hallas, P., et al. (2021). "Microtectonic control of 40Ar/39Ar white mica age distributions in metamorphic rocks (Erzgebirge, N-Bohemian Massif): Constraints from combined step heating and multiple single grain total fusion experiments." Geochimica et Cosmochimica Acta 314: 178–208.
Kroner, U., et al. (2007). The Variscan orogeny in the Saxo-Thuringian zone—Heterogenous overprint of Cadomian/Paleozoic Peri-Gondwana crust. The Evolution of the Rheic Ocean: From Avalonian-Cadomian Active Margin to Alleghenian-Variscan Collision. U. Linnemann, R. D. Nance, P. Kraft and G. Zulauf, Geological Society of America. v. 31: 119.
Mainprice, D., et al. (2011). "Calculating anisotropic physical properties from texture data using the MTEX open-source package." Geological Society, London, Special Publications 360(1): 175–192.
Müller, A., et al. (2011). "Lattice-preferred orientations of late-Variscan granitoids derived from neutron diffraction data: implications for magma emplacement mechanisms." International Journal of Earth Sciences 100(7): 1515–1532.
Yamamoto, Y., et al. (2010). "Extremely Low Magnification EBSD with an FE-SEM." Microsc. Microanal. 16.